Applied Thermal Engineering 111 (2017) 1255–1264

Contents lists available at ScienceDirect

Applied Thermal Engineering

journal homepage: www.elsevier.com/locate/apthermeng

Research Paper

Multiobjective optimization design of green building envelope material using a non-dominated sorting genetic algorithm

Ming-Der Yang [a], Min-Der Lin [b], Yu-Hao Lin [c], Kang-Ting Tsai [d,*]

[a] Department of Civil Engineering, National Chung Hsing University, 250 Kuo-Kuang Rd., Taichung 402, Taiwan
[b] Department of Environmental Engineering, National Chung Hsing University, 250 Kuo-Kuang Rd., Taichung 402, Taiwan
[c] Centre for Environmental Restoration and Disaster Reduction, National Chung Hsing University, 250 Kuo-Kuang Rd., Taichung 402, Taiwan
[d] Program of Landscape and Recreation, National Chung Hsing University, 250 Kuo-Kuang Rd., Taichung 402, Taiwan

HIGHLIGHTS

- An effective envelope energy performance model (BEM) was developed.
- We integrated NSGA-II with the BEM to optimize the green building envelope.
- A tradeoff plan of green building design for three conflict objectives was obtained.
- The optimal envelope design efficiently reduced the construction cost of green building.

ARTICLE INFO

Article history:
Received 24 August 2015
Accepted 6 January 2016
Available online 13 January 2016

Keywords:
Green building
Multiobjective optimization
Nondominated sorting genetic algorithm (NSGA-II)
Building envelope
Energy conservation

ABSTRACT

To realize the goal of environmental sustainability, improving energy efficiency in buildings is a major priority worldwide. However, the practical design of green building envelopes for energy conservation is a highly complex optimization problem, and architects must make multiobjective decisions. In practice, methods such as multicriteria analyses that entail capitalizing on possibly many (but in nearly any case limited) alternatives are commonly employed. This study investigated the feasibility of applying a multiobjective optimal model on building envelope design (MOPBEM), which involved integrating a building envelope energy performance model with a multiobjective optimizer. The MOPBEM was established to provide a reference for green designs. A nondominated sorting genetic algorithm-II (NSGA-II) was used to achieve a tradeoff design set between three conflicting objectives, namely minimizing the envelope construction cost (ENVCOST), minimizing the envelope energy performance (ENVLOAD), and maximizing the window opening rate (WOPR). A real office building case was designed using the MOPBEM to identify the potential strengths and weaknesses of the proposed MOPBEM. The results showed that a high ENVCOST was expended in simultaneously satisfying the low ENVLOAD and high WOPR. Various designs exhibited obvious cost reductions compared with the original architects' manual design, demonstrating the practicability of the MOPBEM.

1. Introduction

Buildings are one of considerable energy consumers, consuming large amounts of energy and releasing considerable amounts of greenhouse gases [1,2]. However, the climate change caused by greenhouse gases emission has an important influence on environmental sustainability [3]. The net-zero energy green building is now seen as the future trend for designing a building [4]. Constructing green buildings involves different building design problems such as orientation choice, façade design, envelope design, thermal comfort, and construction cost [5]; meanwhile, effectively evaluating the thermal performance of building envelopes is crucial work to reduce energy consumption. Several comprehensive building thermal performance simulation models, such as EnergyPlus, TRNSYS, and computational fluid dynamics tools, have been used to facilitate estimating the building energy performance [6–9]. However, using these simulation programs for calculating building envelope energy load (ENVLOAD) has a drawback of longer calculation time and effort to enter detailed building parameters [10,11]. A surrogate program for evaluating the ENVLOAD has been developed by the Taiwanese government to efficiently estimate the air-conditioning cooling load and annual energy performance of building envelopes [12–15]. A low ENVLOAD value indicates low building envelope energy demand and high energy conservation [16], and then the ENVLOAD value was used as a design index for green buildings [13,17].

* Corresponding author.
E-mail address: kttsai@nchu.edu.tw (K.-T. Tsai).

http://dx.doi.org/10.1016/j.applthermaleng.2016.01.015

Building envelope energy performance involves numerous building parameters, including wall insulation, roof insulation, window area, window glazing, window shading, climate zones, and building orientation [18,19]. In other words, designing a green building requires evaluating numerous parameter combinations [20]. Architects typically design building envelope on the basis of their experience and inefficient "trial-and-error" approaches [21]; however, such subjective approaches may not yield optimal results [22]. Therefore, optimizing green building envelopes is a complicated challenge for design teams attempting to counterbalance various conflicting parameters [5]. Lots of optimizers such as genetic algorithm have applied to optimize engineering design and topology of urban building [23–25]. For example, Tuhus-Dubrow et al. coupled a single objective genetic algorithm with EnergyPlus to determine optimal residential building envelope parameters [26]. In practical applications, architects may consider construction costs and other indirect costs such as energy savings as exclusive objectives, and such objectives are frequently conflicting [27]. Typically, the approach to resolve multiobjective optimization problems involves combining multiple objectives into a single composite function by adaptive weights; however, determining the weight is dependent on the required prior knowledge and the result does not provide information about the compromise between the objectives [5]. Another approach entails using a multiobjective algorithm to determine a set of optimal solutions that are nondominated with respect to each other, called "Pareto front (PF)" solutions. A PF embodies a tradeoff between conflicting objectives. The nondominated sorting genetic algorithm-II (NSGA-II) is one of the most prevalent multiobjective optimizers involving discrete integer and hybrid variables [5]. Then, Evins et al. employed the NSGA-II to optimize the cost and energy use of a modular building [27,28].

An optimization of the building envelope is required to achieve a high energy performance of the building [29], and a practical building envelope design usually should consider multiobjective. None of studies conducted multiobjective optimization for building envelope designs in Taiwan, and an efficient energy simulation model based on the ENVLOAD to estimate a building energy demand is rare. The current study integrated NSGA-II with a building envelope energy estimation model (BEM) to create a multiobjective optimal BEM decision support system (MOPBEM) for designing green building envelopes. The developed BEM was derived from the ENVLOAD, and the MOPBEM was validated in a real building design case. The NSGA-II was employed to achieve a tradeoff between two or among three conflicting objectives of building envelope design, namely minimizing the envelope construction cost (ENVCOST), minimizing the building energy demand (ENVLOAD), and maximizing the façade window opening rate (WOPR). Because the original design case considered the ENVCOST under a constant WOPR and ENVLOAD constraint, the MOPBEM were firstly executed for only two objectives (ENVCOST and ENVLOAD) to obtain an optimal design that was compared with the original design to demonstrate the validation of MOPBEM. Meanwhile, the parameter sensitivity analysis in NSGA-II was investigated to demonstrate the robustness of this algorithm. However, usually two objectives in practical could not meet architects' request. Consequently, the MOPBEM was used to investigate different design scenarios for these three objectives.

2. Methodology

2.1. BEM and NSGA-II

Fig. 1 illustrates a schematic of the BEM, indicating that the building envelope configuration comprises several main components: window glass, wall, glass curtain, roof, and window sunshades. The building ENVLOAD (Wh/m^2/yr) used in this study was related to sunlight, climate, building orientation, envelope configuration, and air-

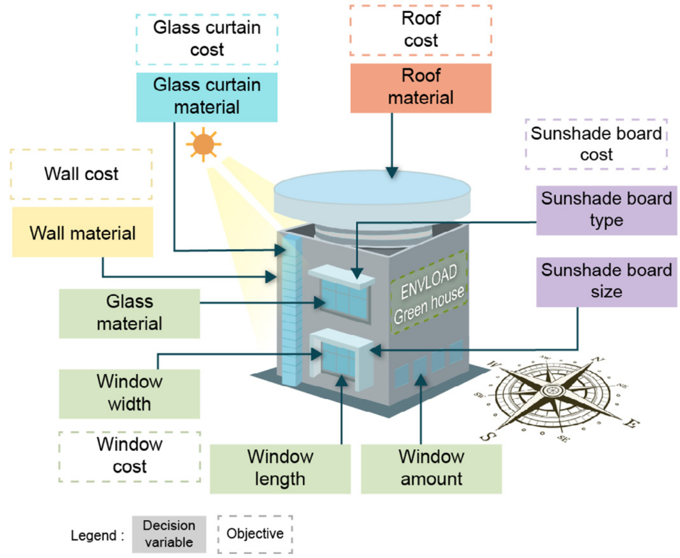

Fig. 1. Conceptual illustration and components for building envelope, construction cost, and ENVLOAD in the MOPBME.

conditioner use. As shown in Fig. 1, nine design variables (decision variable) were used in the BEM for estimating the ENVLOAD: the number of windows, window length, window width, window glass material, wall material, glass curtain material, roof material, sunshade type, and sunshade board size. Specifically, the construction cost of building envelopes are functions of the window area, window glass material, sunshade board size, wall material, roof material, and glass curtain materials. Furthermore, the ENVLOAD of a building envelope involves climate conditions; the climatic zones in Taiwan were divided into north, central, and south zones (Fig. 2). The ENVLOAD for green building in Taiwan has various standard levels, and the climate of building case located in the south zone has relatively different cooling degree and insolation hours from that located in the north zone.

Fig. 3 depicts a flowchart of the BEM. First, the constant and basic data for constructing a building are collected. After the main architectural structure and building orientation are preplanned, an architect should classify the building envelope into various components and sectors in the kth building orientation (Fig. 2). Constant data for estimating an ENVLOAD, including floor area and building location, are input to the model. Decision variables for an ENVLOAD, such as envelope configuration material, sunshade size, sunshade type for each building sector in dissimilar orientations, are determined and input. Subsequently, the required ENVLOAD components, including window area, solar transmittance, and envelope thermal conductance, is derived directly. Three sunshade options, namely horizontal, vertical, and grid sunshade, are available in the BEM, and the sunshade effect depends on factors such as the building orientation and window size. Specifically, the coefficient of the sunshade effect (K_i) for the window in the ith sector is estimated by evaluating the depth rate of the sunshade board, sunshade type, and building façade orientation. Next, in the ith sector, the insolation gain and heat loss coefficient, Mk_i and L_i, are calculated for the air-conditioned and nonair-conditioned zones, respectively. The cooling degree and insolation hours, DH and IHk, respectively, are determined according to the building orientation and location. Concurrently, the window area and wall area in each orientation are estimated. Finally, the ENVLOAD value is calculated using Eq. (1), and is a function of Mk_i, L_i, DH, and IHk [13]. The ENVLOAD for various building categories has different annual indoor heat gain (G) and regression coefficient [13–15].

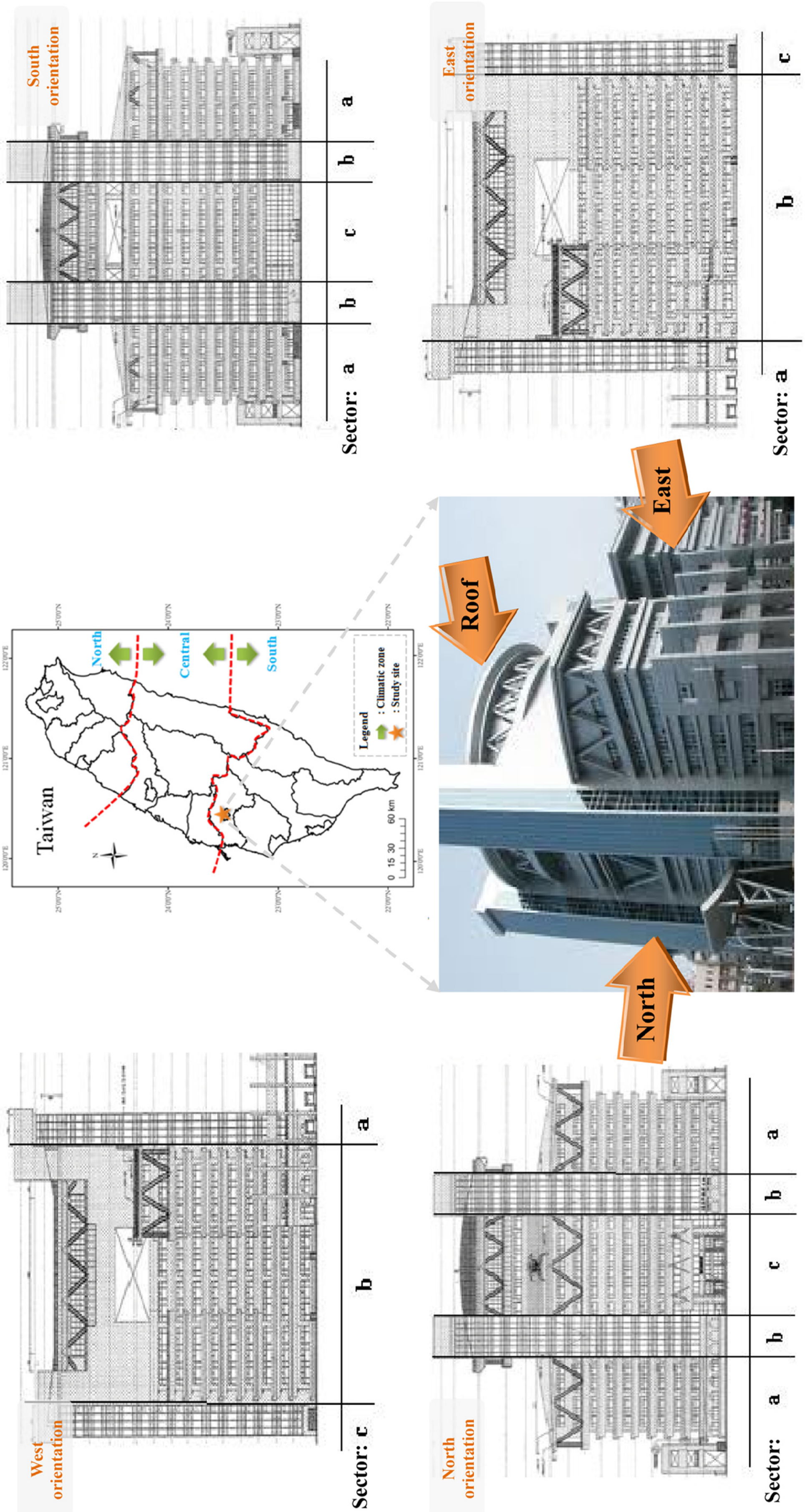

Fig. 2. Climatic zones in Taiwan and layout of the case study building in different orientations.

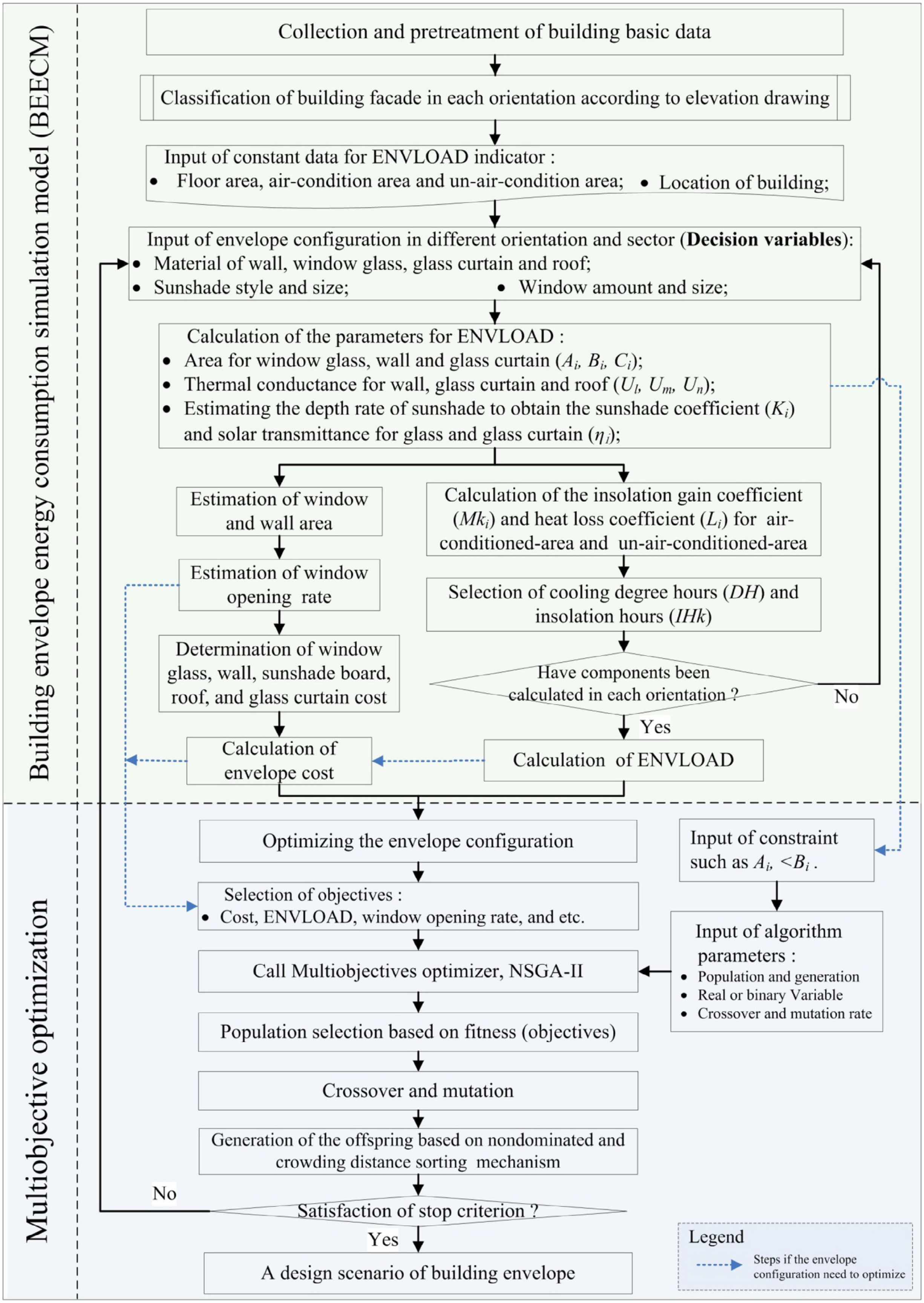

Fig. 3. Flowchart of the MOPBME model.

The BEM can be formulated as shown in Eqs. (1)–(17), and the *WOPR* and shadow area of this building can be calculated:

$$ENVLOAD = a_0 + a_1 \times \sum_k^{No} G + a_2 \times \sum_k^{No} (L_i \times DH) + a_3 \times \sum_k^{No} (Mk_i \times IHk) \quad (1)$$

$$L_i = 1.011 + \left\{ \{U_l \times \sum_i^{Nsi} (B_i - B_i' - A_i) + U_m \times \sum_i^{Nsi} (C_i - C_i') + U_n \times (D - D') + 0.5 \times \left[U_l \times B_i' + U_m \times \sum_i^{Nsi} C_i' + U_n \times D' \right] \right\} \Big/ AFp \quad (2)$$

$$Mk_i = (Vaira + Vunaira)/AFp \quad (3)$$

$$Vaira = \sum_i^{Nsi} (K_i \times \eta_i \times A_i) + 0.035 \times \left[U_l \times \sum_i^{Nsi} (B_i - B_i' - A_i) \right] + 0.035 \times [U_n \times (D - D')] \quad (4)$$

$$Vunaira = 0.5 \times \left[0.035 \times U_l \times \sum_i^{Nsi} B_i' \right] + 0.035 \times U_m \times \sum_i^{Nsi} C_i' + 0.035 \times U_n \times D' \Big] \quad (5)$$

$$A_i = WINDN_i \times WINDL_i \times WINDW_i \quad (6)$$

$$K_i = F(SUNSHS_i, depthrate, k) \quad (7)$$

$$E_i = F(WINDN_i, WINDW, SUNSHS_i, SUNSHL_i) \quad (8)$$

For horizontal sunshade type (if $SUNSHS_i = 1$),

$$depthrate = SUNSHL_i / WINDW_i \quad (9)$$

$$E_i = WINDN_i \times WINDW_i \times SUNSHL_i \quad (10)$$

For vertical sunshade type (if $SUNSHS_i = 2$),

$$depthrate = SUNSHL_i / WINDL_i \quad (11)$$

$$E_i = WINDN_i \times WINDL_i \times SUNSHL_i \times 2 \quad (12)$$

For grid sunshade type (if $SUNSHS_i = 3$),

$$depthrate = (SUNSHL_i / WINDW_i + SUNSHL_i / WINDL_i)/2 \quad (13)$$

$$E_i = WINDN_i \times WINDW_i \times SUNSHL_i + WINDN_i \times WINDL_i \times SUNSHL_i \times 2 \quad (14)$$

$$WOPR = WAREA/BFAREA \quad (15)$$

$$WAREA = \sum_k^{No} \sum_{i=1}^{Nsi} (A_i + A_i') \quad (16)$$

$$BFAREA = \sum_k^{No} \sum_{i=1}^{Nsi} (A_i + A_i' + B_i + B_i' + C_i' + C_i') \quad (17)$$

Here, $WINDN_i$, $WINDW_i$, $WINDL_i$, $SUNSHL_i$, and $SUNSHS_i$ are the design variables that represent window number, window unit width, window unit length, sunshade board unit length, sunshade style, respectively. *No* is the number of building orientations; Ns_i is the number of sectors in the *i*th building orientation. a_0 is a constant, where a_1, a_2, and a_3 are regression coefficients; these constant and coefficients are depended on the building type. *G* is the annual indoor heat gain (Wh/m^2/yr) and depends on the building category. The product of L_i and *DH* represents the heat loss of the building construction material, Mk_i is the insolation gain coefficient of the envelope in the *i*th sector (Wh/m^2/K), and the product of ΣMk_i and *IHk* represents the heat gain and involves the sunshade factor. The areas of the window glass, wall, glass curtain, and roof in the air-conditioned and nonair-conditioned zones in the *i*th sector are denoted as A_i and A_i', B_i and B_i', C_i and C_i', and D_i and Di', respectively (m^2); η_i is the solar transmittance of the glass, and U_l, U_m, and U_n are the thermal conductance of the wall, glass curtain, and roof, respectively (W/m^2/K). Furthermore, *AFp* (m^2) is the area of surrounding regions 5 m from the building boundary to the center of the building interior [16,30]. $SUNSHS_i$ represents the sunshade type in the *i*th sector; the sunshade board length in the *i*th sector is denoted as $SUNSHL_i$, and the number, length, and width of the window in the *i*th sector are denoted as $WIND_i$, $WINDL_i$, and $WINDW_i$, respectively. *WAREA* and *EBAREA* represent the areas of the window and building envelope in the façade. In addition, *ENVCOST* is the sum of the costs of the window, window glass material, sunshade board, and wall, roof, and glass curtain materials of the building envelope (Fig. 1). These data of available materials used to building envelope, including the thermal conductance, solar transmittance, and cost, were shown in Tables S1–S4 in the Supplementary Material.

2.2. Case study

An office building in Chiayi City in Southern Taiwan, located at an altitude of 30 m, was designed to validate the feasibility of MOPBEM. Fig. 2 illustrates a photograph of the office building and the façade in various orientations. In a orientation, the envelope façade can be divided into three sectors (a, b, and c) to determine the design variables in the MOPBEM. This office building comprises 13 aboveground floors and windows equipped with horizontal sunshade boards; Tables 1 and 2 list other essential data and original

Table 1
Basic data and original design for study case building.

Envelope area (m^2)	Category	Orientation	South	East	North	West
	Wall and window	A_i[a]	0.0	419.7	0.0	419.7
		NA_i[b]	261.9	1124.1	227.4	1124.1
	Glass curtain	A_i	1532.0	1525.2	1772.7	1525.5
		NA_i	1138.8	1264.5	1173.3	1264.5
	Roof	A_i	2893.3			
		NA_i	531.5			
	Total, *BFAREA*		19,007.5			
Total surroundings area[c], *AFp* (m^2)						13,139.5
Air conditioner operation time, *Ac* (hour/yr)						1885.5
Annual average internal loads, *G* (Wh/m^2/yr)						25,453.5
Degree-hours based on monthly temperature averages , *DH* (Kh/yr)						16,100
Coefficient of heat loss of the envelope, *L* (Wh/m^2/K)						6.72
Number of floors						13

[a] : air-conditioned-zone; [b] : non-air-conditioned-zone; [c] : *AFp* is the area of the region between 5 m from the building boundary and the center of the building interior.

Table 2
Original and optimal design at similar ENVLOAD and WOPR values.

Building	Scenario	Original design				Optimal design			
Orientation	Sector	Sunshade board			Window	Sunshade board			Window
		Style	Number	Size+	Open rate* (%)	Style	Number	Size+	Open rate* (%)
North	a (front)	Horizontal	16	1 × 1.6	21.2	Vertical	8	2.0 × 2.4	21.4
	c	Horizontal	22	1 × 1.6		Vertical	6	2.0 × 2.0	
	a (back)	Horizontal	7	1 × 1.6		Vertical	1	1.2 × 1.2	
East	a and c	Horizontal	10	1 × 1.6	11.5	Horizontal	4	1.6 × 2.8	11.5
	b	Horizontal	16	1 × 1.6		Horizontal	6	1.8 × 2.0	
South	a (front)	Horizontal	16	1 × 1.6	20.0	Grid	9	1.6 × 2.6	20.0
	c	Horizontal	22	1 × 1.6		Vertical	10	1.6 × 1.4	
	a (back)	Horizontal	7	1 × 1.6		Grid	1	1.8 × 1.4	
West	a and c	Horizontal	10	1 × 1.6	11.5	Horizontal	3	2.0 × 2.4	11.6
	b	Horizontal	16	1 × 1.6		Horizontal	8	1.4 × 2.6	
ENVLOAD (Wh/m²/yr)		87.45				87.75			
Total widow area (m²)		3071				3084			
Sunshade board area (m²)		3075.2				1550.0			
Envelope cost ($NTD*)		61,856,720				36,005,350			
Cost reduction ratio (%)		-				47.1			

* New Taiwanese Dollar; + : length × width (m), and the length is design variable and width is constant; *: window area/wall area.

design of the envelope. The wall area is relatively low in the southern and northern façades, and the heat loss of the envelope (L) and annual air-conditioner operation time (Ac) in the original design is 16100 Wh/m$_2$/yr and 1885.5 hrs, respectively. Table 3 lists the *DH and IHk* coefficients in different climatic zones; the *IHk* value in the northern climatic zone decreased compared with that in the southern climatic zone, indicating that Taiwan is characterized by high climatic variations. Table S1 in the Supplementary Material lists the coefficient of the sunshade effect, K_i, for this study case. Tables 1 and 2 show the original design plan, derived from the BEM, of the case building. The estimated ENVLOAD value and building envelope cost were 87.45 KWh/m^2/yr and 61.86 million New Taiwan dollars ($NTD), respectively; although this ENVLOAD satisfies the energy conservation regulations for green buildings in Taiwan (<92 KWh/m^2/yr). The WOPRs in the northern, eastern, southern, and western orientations were 21.2%, 11.5%, 20.0%, and 11.5%, respectively. Lower construction cost would be obtained using the MOPBEM, and a cost effectiveness analysis and two design scenarios for the study case were investigated.

2.3. NSGA-II and MOPBEM

As illustrated in Fig. 3, the first section in the MOPBEM is implementing the BEM to obtain the building ENVLOAD and construction cost. To design an optimal building envelope configuration, NSGA-II is implemented when architects determine their preferred objectives and construction constraints. The NSGA-II is mainly based on a nondominated sorting (NDS) and crowding distance sorting mechanisms. Such mechanisms ensure both the convergence of the population and its spread; the major procedures include population generation, population fitness evaluation, population ranking according to crowding distance, elitist selection, bimodal crossover, and mutation. The detail NSGA-II procedures including the Selection could also refer to the Alinia Kashani et al. study [31]. Parent populations are ranked into an NDS order and used to form a new offspring [32]. The NSGA-II input parameters include the population size, number of generations, mutation probability, crossover probability, and number of objectives. Some of these parameters are used in conducting a sensitivity analysis to demonstrate their effect on the tradeoff solution.

Objectives in the MOPBEM can be set as a function of a quantifiable direct cost or an indirect cost such as energy demand. The mentioned design variables in the BEM (as shown in Fig. 1), including number of windows, window length, window width, window glass material, wall material, glass curtain material, roof material, sunshade type, and sunshade board length, serve as decision variables in the MOPBEM. For the study case, three conflicting objectives were evaluated and are sequentially outlined as follows: to minimize the *ENVCOST*, minimize the *ENVLOAD*, and maximize the *WOPR*. A high *WOPR* may result in a high solar gain, day lighting, and ventilation for a building. Compared with the first objective, the second objective is associated with environmental costs and has the monetized difficulty; typically, a low *ENVLOAD* and high *WOPR* are incompatible with low envelope construction costs. The detailed mathematical formulation of MOPBEM is expressed as shown in Eqs. (2)–(25):

Minimize *ENVCOST*:

$$\begin{aligned} ENVCOST &= \sum_{k}^{No}\sum_{i}^{Nsi}(A_i + A_i') \times WGLCOST + \sum_{k}^{No}\sum_{i}^{Nsi}(B_i + B_i') \\ &\times WALCOST_l + \sum_{k}^{No}\sum_{i}^{Nsi}(C_i + C_i') \times GLCUCOST + \sum_{k}^{No}\sum_{i}^{Nsi}E_i \\ &\times SUNSHDCOST + (D_i + D_i') \times ROFCOST \end{aligned} \quad (18)$$

Table 3
ENVLOAD parameters in various climatic zones and orientations.

Climatic zone			Southern	Northern
Insolation hours, IHk (h/yr)	Horizontal plane (i.e. Roof)		1,039,000	695,900
	Vertical plane	South	464,500	273,800
		West	564,000	177,000
		North	267,000	276,400
		East	392,700	314,000
ENVLOAD standard for green building (kWh/m²/yr)			92	64
Cooling degree, *DH* (Kh/yr)			16100	12200
Cooling air-conditioning hours, *Ac* (h/yr)			$1661 + 118 \times Tu^{*} - 3.1 \times Tu^2$	$1198 + 111 \times Tu$

* : $Tu = 13.5/L$, L is heat loss coefficient of the building envelope.

Minimize *ENVLOAD*:

$$ENVLOAD = 120370 + 2.01 \times \sum_{k}^{No} G + 0.033 \times \sum_{k}^{No} (L_i \times DH) + 1.079 \times \sum_{k}^{No} (Mk_i \times IHk) \quad (19)$$

Maximize *WOPR*:

$$WOPR = WAREA/BFAREA \quad (20)$$

For office building,

$$G = 13.5 \times Ac \quad (21)$$

$$Ac = 1661 + 118 \times Tu - 3.1 \times Tu^2 \quad (22)$$

$$Tu = \frac{13.5}{L} \quad (23)$$

Subject to:

$$WINDN_i \times WINDW_i \leqq FLOORW_i \quad (24)$$

$$ROGWOPR \leq WOPR \quad (25)$$

In these equations, *WGLCOST*, *WALCOST*, *GLCUCOST*, *ROFCOST*, and *SUNSHDCOST* are the unit costs of the window glass, wall, glass curtain, roof, and sunshade board, respectively; these costs depend on the design variables, including sequentially glass material, wall material, glass curtain material, roof material, and sunshade board material, respectively; the unit price and property of these material was shown in Table S2–S5 (in the Supplementary Material). E_i represents the areas of the sunshade board in the ith sector and is a function of the window size, sunshade type, and sunshade board length. Furthermore, *Ac* is the air-conditioning hours (h/yr) and is a function of location and altitude and *Tu* is the increment in the average room temperature of the building (K); for the study case, *No* and *Nsi* were 4 and 3, respectively (Fig. 2). $FLOORW_i$ represents the floor width in the ith sector. *ROGWOPR* is the original design WOPRs of the building envelope. If the third objective of maximizing *WOPR* is evaluated, Eq. (24), the WOPR constraint, can be ignored.

Table 4 shows the decision variables, and components of objectives and ENVLOAD in the MOPBEM; the nine categories of decision variable were coded in NSGA-II. For example, the codes for the sunshade type can be expressed as follows: 1 (horizontal sunshade), 2 (vertical sunshade), and 3 (grid sunshade). The window glass, wall, roof, and glass curtain materials can be coded as 1 to the material candidate number, for which the candidate numbers of the glass, wall, and roof are 58, 23, and 19, respectively. The fitness of the chromosome in NSGA-II is expressed according to the objective values. Other decision variables are directly encoded as integer numbers representing the number of unit lengths, and the actual window size is the product of the number and unit length. All computational code routines were coded in Fortran programming language and ran on a personal computer equipped with 8 GB of RAM and an Intel i5 processor running at 3.2 GHz. Finally, the MOPBEM product is a tradeoff curve for design reference.

Table 4
Objective and discrete decision variable representation in the MOPBEM.

Components of the objective	Design (decision) variable (nomenclature)	Option value
ENVLOAD, window opening rate and cost	Window number (*WINDN$_i$*)	[1, L][a]
	Window unit width (*WINDW$_i$*)	[6, 12]
	Window unit length (*WINDL$_i$*)	[6, 14]
	Glass material	[1, 58][b]
ENVLOAD and sunshade board cost	Sunshade board unit length (*SUNSHL$_i$*)	[3, 18]
	Sunshade style (*SUNSHS$_i$*)	[1, 3][c]
	Sunshade board material	[1, 23][b]
ENVLOAD and wall cost	Wall material	[1, 23][b]
ENVLOAD and roof cost	Roof material	[1, 19][b]
ENVLOAD and glass curtain cost	Glass curtain material	[1, 5][b]

[a] : L changes with the azimuth of building; [b] : refer to tables in supplementary material; [c] : 1, 2, and 3 indicates the horizontal, vertical, and grid sunshade, respectively.

3. Results and discussion

3.1. Multiobjective optimal design and cost effectiveness analysis

For the study case, 54 design variables were evaluated in the MOPBEM. The solution space comprised approximately 2.38×10^{50} possible designs, and discrete variables make the optimization problem nonconvex and discontinuous, both implying that resolving this optimal design set is difficult [33] and [34]. To investigate the robustness of the NSGA-II, several MOPBEM runs were executed using various NSGA-II parameters and a similar WOPR to the original design, in which these parameters used the same crossover rate of 0.85 and mutation rate of 0.05, but different population (P) and generation (G) sizes. Fig. 4 depicts the optimal tradeoff solutions (designs) for two objectives, namely minimizing the construction cost and minimizing the ENVLOAD. The PF comprised the optimal tradeoff solutions, and each of these solutions represented a design associated with a minimum ENVLOAD at a specific envelope cost. As expected, simultaneously reducing the building energy demand (ENVLOAD) increased the construction cost; most of the envelope materials in the Pareto solution set has low thermal conductivity, thus leading to a lower building load coefficient and consequently higher energy savings that result in high cost [35].

The number of feasible solutions increased with the generations because of the evolution and propagation of optimal chromosomes. Moreover, these solutions clearly converged to a PF, and the number of generations to obtain a PF was depended on the population number. The second tradeoff curve (Fig. 4, orange dots) was observed using a population size of 500 after 100 evolution generations; if the generation of this evolution was continued to 250 generations, a relatively inefficient evolution was derived, which had a limited improvement on the solution and emphasized on generating an extreme solution such as the lowest ENVLOAD. Compared with the result of a large population size (P = 500), the low populations size (P = 100) required more generations to generate Pareto solutions, but such solutions did not approach the optimal PF (Fig. 4, brown dots). Specifically, for this case, a large population was more efficient than a large generation in enhancing the optimal PF product. Such parameter set specifications for evolutionary algorithms may depend on the request in various generation stages for each problem [36,37].

Overall, the estimated construction cost ranged from 35 million to 79 million NTD, depending on the requested ENVLOAD. The maximum benefit-to-cost ratios ranged between 80 and 90 (Wh/m^2/yr). In other words, the required ENVLOAD of the case building can be set at 80 (Wh/m^2/yr) under a limited construction budget. When the ENVLOAD value was lower than 56, the construction budget of the sunshade board increased drastically to reduce the solar heat gain through windows. Table 2 shows an optimal envelope configuration design with the approximate ENVLOAD value (87.75), which is similar to that of the original design (87.45). The cost was reduced by approximately 25.85 million NTD (47.1%) compared with the original architects' manual design, signifying that the NSGA-II satisfactorily solves the envelope multiobjective optimization problem. This result also demonstrated that using highly

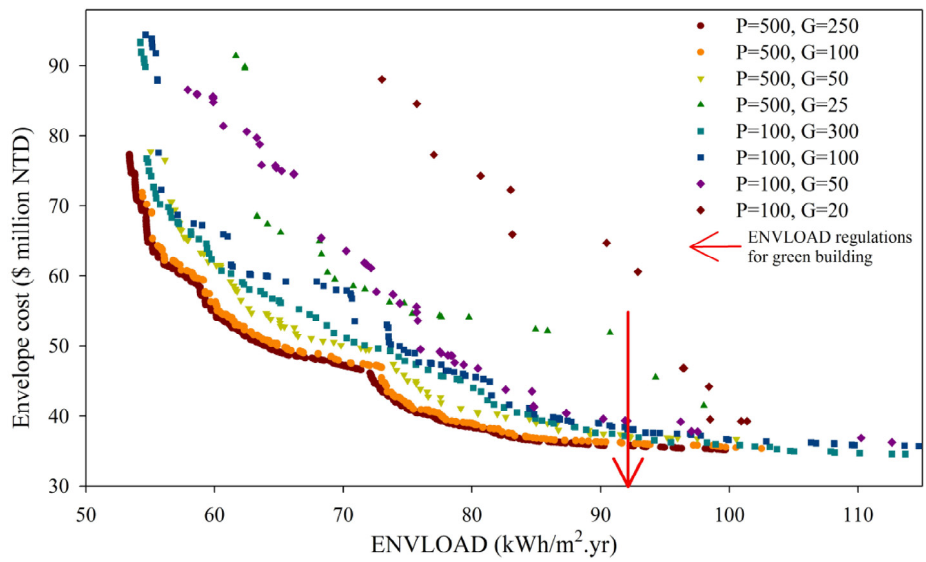

Fig. 4. Pareto front calculated from various NSGA-II parameters. (For interpretation of the references to color in citations to this figure, the reader is referred to the web version of this article.)

expensive and frequently recommended envelope materials is unnecessary in constructing green buildings.

Design variables, including number of windows, window length, window width, sunshade type, and sunshade board length, in optimal design was shown in Table 2. Compared with the original design, the optimal design involved fewer numbers of windows and larger window sizes with diverse types of sunshade. A lower sunshade coefficient (K_i) indicates higher sunshade efficiency for windows, and the sunshade effect depends on the building orientation, sunshade type, and sunshade board length. That vertical sunshades have high sunshade efficiency was observed in Table S1 (in the Supplementary Material) because of high variations in sunshade coefficients. Meanwhile, vertical sunshades have lower construction cost compared with grid sunshades. Therefore, vertical sunshades are used in all windows in the northern orientation to efficiently reduce incident sunlight in this case. By contrast, numerous grid sunshades are used in the southern orientation to increase sunshade effects because they yield the highest variation in sunshade coefficients in this orientation. The obvious decrease in the sunshade board area also depicted that the optimal design exhibited a more favorable shade effect compared with the original design. Other design variables, including window glass material, wall material, glass curtain material, roof materials, in original and optimal design was listed in Table S6. Except for the wall material with higher thermal transmittance, but lower cost, the material configurations in optimal design entail lower unit cost and thermal transmittance compared with the original design. These results revealed that optimized sunshade designs efficiently facilitate reducing the solar heat gain through windows and the sunshade board area, thus reducing envelope costs. According to the aforementioned results, the MOPBEM can offer a complete building envelope design set for architects' reference.

3.2. Scenario I: tradeoff design for three objectives

The optimal design, which restricts the WOPR and excludes the external building outlook, may be unrealistic and not meet architects' request. Consequently, this optimization set contains three conflicting objectives, namely *ENVCOST*, *ENVLOAD*, and *WOPR*. Fig. 5 illustrates the optimal tradeoff solutions for these conflicting objectives. These solutions were obtained using a population size of 500 and 250 generations. These Pareto tradeoff solutions formed a three-dimensional (3D) Pareto surface (PS). Obviously, the PS for southern zone of the study case exhibited ENVLOAD values ranging from 39 to 110 (Wh/m^2/yr), envelope cost between 35 million and 90 million NTD, and a WOPR ranging from 3% to 25%. As expected, a high ENVCOST was incurred in simultaneously satisfying the low energy demand and high WOPR requirements. A lower WOPR implies lower solar gain and higher energy performance; therefore, the required ENVLOAD can be achieved using only higher thermal conductance envelope materials with lower cost. Furthermore, the 3D PS provided a complete representation of the conflicting features in the objective function space as well as the tradeoff among the various designs to be visualized for design reference.

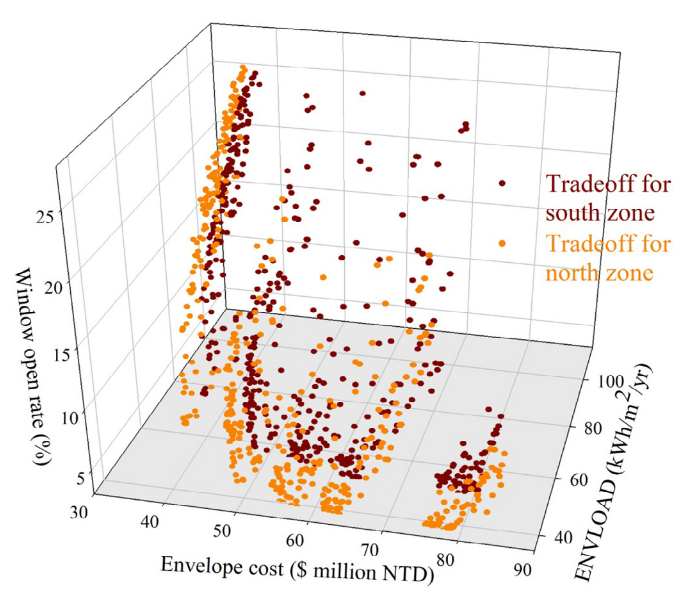

Fig. 5. Difference in tradeoff between southern and northern climatic zones.

3.3. Scenario II: tradeoff curve for different climatic zones

The goal of this scenario was to investigate the effect of climatic zones on green building designs. The north tropic of Cancer (23.5° N) runs across the middle section of Taiwan, and brings the tropical monsoon climate in the south and the subtropical monsoon climate in the north. High temperature and humidity, massive rainfall and gusty winds characterize the climate of Taiwan. For example, average temperature is approximately 20, 23.5 and 27 °C in the northern, central, and southern metropolis during 1997–2010. The climatic differences of different zones must be taken into consideration, and the ENVLOAD standards come in three groups corresponding to northern, central, and southern Taiwan. Table 3 shows several ENVLOAD parameters in various climatic zones and orientations, and the study case was optimized based on these different parameters, which include *DH*, *IHk*, and *Ac*. Fig. 5 depicts the two PSs for various climatic zones, indicating that a low ENVLOAD design requires high construction costs. At the approximate construction cost and WOPR, the ENVLOAD designed for the southern zone was generally higher than that for the northern zone at the approximate construction cost and WOPR. To achieve the same ENVLOAD, the window area (i.e., WOPR) designed for the southern zone was smaller than that for the northern zone according to an approximate construction cost. These results are attributable to the longer *IHk* in the southern zone than that in the northern zone, in which the *IHk* indicated that the building possibly had a higher thermal gain and that the climate of the southern zone was hotter than that of the northern zone. Specifically, when two similar buildings located in the northern and southern zones are constructed with the same budget, the building in the southern zone may demonstrate a higher ENVLOAD than that in the northern zone. This result is also consistent with that different climatic zones have different regulatory standards of ENVLOAD for green buildings; therefore, Table 3 shows that the regulatory standards of ENVLOAD for green buildings in the southern and northern zones are 92 and 64 (Wh/m^2/yr), respectively.

4. Conclusions

The design of low-energy green buildings has attracted increasing attention in both academic and professional fields, and energy simulation of building envelopes is indispensable for green building design. A simplified building energy demand, ENVLOAD, serving as a green building index was proposed in Taiwan. However, building envelope design considering conflicting multiobjective in practical applications is a highly nonlinear and nonconvex optimization problem. Therefore, this study proposes an optimal MOPBEM, which involves integrating the energy simulation of building envelopes with multiobjective optimizers, for decision-making reference. The NSGA-II is used to achieve a tradeoff between two or three conflicting objectives, namely minimizing the building ENVCOST, minimizing the building ENVLOAD, and maximizing the building WOPR. A building in Chiayi City in Southern Taiwan was investigated to demonstrate the feasibility of the proposed MOPBEM. Two NSGA-II parameters, namely the population size and number of generations, were determined thorough a sensitivity analysis to investigate their effects on the optimal tradeoff solution and the robustness of the NSGA-II.

As expected, high ENVCOST was incurred in simultaneously satisfying low energy demand and high WOPR requirements. Because a lower WOPR indicates a lower thermal energy gain of a building, the required ENVLOAD can be achieved using higher thermal conductance envelope materials with lower cost, resulting in a lower construction cost. One of the tradeoff designs exhibited a cost reduction of 47.1% compared with the original architects' manual design, demonstrating the feasibility of the proposed MOPBEM. The PS result revealed that buildings with the same envelope design but located in different climatic zones may demonstrate clear differences in energy performance because of the difference in insolation hours. Summarily, those tradeoff solutions calculated from the MOPBEM can serve as a reference for establishing regulatory standards of green building energy performance in various climatic zones.

Acknowledgements

The authors would like to thank the National Science Council of Taiwan for the partial financial support for this research under Project NSC100-2221-E-507-005 and NSC-102-2221-E-005-003-MY3. This work is also supported in part by the Ministry of Education, Taiwan, under the ATU plan.

Appendix: Supplementary material

Supplementary data to this article can be found online at doi:10.1016/j.applthermaleng.2016.01.015.

References

[1] C.A. Balaras, K. Droutsa, E. Dascalaki, S. Kontoyiannidis, Heating energy consumption and resulting environmental impact of European apartment buildings, Energy Build. 37 (2005) 429–442.
[2] A.M. Omer, Energy, environment and sustainable development, Renew. Sustain. Energy Rev. 12 (2008) 2265–2300.
[3] C. Endler, K. Oehler, A. Matzarakis, Vertical gradient of climate change and climate tourism conditions in the Black Forest, Int. J. Biometeorol. 54 (2010) 45–61.
[4] A.J. Marszal, P. Heiselberg, J. Bourrelle, E. Musall, K. Voss, I. Sartori, et al., Zero energy building – a review of definitions and calculation methodologies, Energy Build. 43 (2011) 971–979.
[5] V. Machairas, A. Tsangrassoulis, K. Axarli, Algorithms for optimization of building design: a review, Renew. Sustain. Energy Rev. 31 (2014) 101–112.
[6] L. Bellia, F. De Falco, F. Minichiello, Effects of solar shading devices on energy requirements of standalone office buildings for Italian climates, Appl. Therm. Eng. 54 (2013) 190–201.
[7] G. Pagliarini, C. Corradi, S. Rainieri, Hospital CHCP system optimization assisted by TRNSYS building energy simulation tool, Appl. Therm. Eng. 44 (2012) 150–158.
[8] W. Pasut, M. De Carli, Evaluation of various CFD modelling strategies in predicting airflow and temperature in a naturally ventilated double skin façade, Appl. Therm. Eng. 37 (2012) 267–274.
[9] A. Buonomano, F. Calise, G. Ferruzzi, L. Vanoli, A novel renewable polygeneration system for hospital buildings: design, simulation and thermo-economic optimization, Appl. Therm. Eng. 67 (2014) 43–60.
[10] D. Gossard, B. Lartigue, F. Thellier, Multi-objective optimization of a building envelope for thermal performance using genetic algorithms and artificial neural network, Energy Build. 67 (2013) 253–260.
[11] G.H. dos Santos, N. Mendes, Analysis of numerical methods and simulation time step effects on the prediction of building thermal performance, Appl. Therm. Eng. 24 (2004) 1129–1142.
[12] K.H. Yang, R.L. Hwang, The analysis of design strategies on building energy conservation in Taiwan, Build. Environ. 28 (1993) 429–438.
[13] K.-H. Yang, R.-L. Hwang, An improved assessment model of variable frequency-driven direct expansion air-conditioning system in commercial buildings for Taiwan green building rating system, Build. Environ. 42 (2007) 3582–3588.
[14] K.-T. Huang, H.-T. Lin, Design standard of energy conservation for building HAVC-a simplified method of chiller capacity estimation based on building envelope energy conservation index in Taiwan, 2005.
[15] K.-T. Huang, H.-T. Lin, Development of simplified estimation method of chiller energy use for office buildings in Taiwan, ASHRAE Trans. 113 (2007).
[16] R.-L. Hwang, S.-Y. Shu, Building envelope regulations on thermal comfort in glass facade buildings and energy-saving potential for PMV-based comfort control, Build. Environ. 46 (2011) 824–834.
[17] Y. Huang, J.-L. Niu, Energy and visual performance of the silica aerogel glazing system in commercial buildings of Hong Kong, Constr. Build. Mater. 94 (2015) 57–72.
[18] M. Sahu, B. Bhattacharjee, S.C. Kaushik, Thermal design of air-conditioned building for tropical climate using admittance method and genetic algorithm, Energy Build. 53 (2012) 1–6.
[19] A. Alaidroos, M. Krarti, Optimal design of residential building envelope systems in the Kingdom of Saudi Arabia, Energy Build. 86 (2015) 104–117.
[20] P. Aparicio Ruiz, J. Guadix Martín, J.M. Salmerón Lissén, F.J. Sánchez de la Flor, An integrated optimisation method for residential building design: a case study in Spain, Energy Build. 80 (2014) 158–168.
[21] X. Shi, Design optimization of insulation usage and space conditioning load using energy simulation and genetic algorithm, Energy 36 (2011) 1659–1667.
[22] Y. Bichiou, M. Krarti, Optimization of envelope and HVAC systems selection for residential buildings, Energy Build. 43 (2011) 3373–3382.

[23] M.-D. Yang, A genetic algorithm (GA) based automated classifier for remote sensing imagery, Can. J. Remote Sens. 33 (2007) 203–213.

[24] M.-D. Yang, T.-C. Su, An optimization model of sewage rehabilitation, J. Chin. Inst. Eng. 30 (2007) 651–659.

[25] C.A. Conceição António, J.B. Monteiro, C.F. Afonso, Optimal topology of urban buildings for maximization of annual solar irradiation availability using a genetic algorithm, Appl. Therm. Eng. 73 (2014) 424–437.

[26] D. Tuhus-Dubrow, M. Krarti, Genetic-algorithm based approach to optimize building envelope design for residential buildings, Build. Environ. 45 (2010) 1574–1581.

[27] R. Evins, A review of computational optimisation methods applied to sustainable building design, Renew. Sustain. Energy Rev. 22 (2013) 230–245.

[28] R. Evins, P. Pointer, R. Vaidyanathan, S. Burgess, A case study exploring regulated energy use in domestic buildings using design-of-experiments and multi-objective optimisation, Build. Environ. 54 (2012) 126–136.

[29] J. Mazo, A.T. El Badry, J. Carreras, M. Delgado, D. Boer, B. Zalba, Uncertainty propagation and sensitivity analysis of thermo-physical properties of phase change materials (PCM) in the energy demand calculations of a test cell with passive latent thermal storage, Appl. Therm. Eng. 90 (2015) 596–608.

[30] H.-T. Lin, J.-C. Wang, The design index of building energy conservation and CAD program BEEP in Taiwan, in: Proceedings of the Eighth International IBPSA Conference, August, 2003, pp. 11–14.

[31] A.H. Alinia Kashani, A. Maddahi, H. Hajabdollahi, Thermal-economic optimization of an air-cooled heat exchanger unit, Appl. Therm. Eng. 54 (2013) 43–55.

[32] K. Deb, A. Pratap, S. Agarwal, T. Meyarivan, A fast and elitist multiobjective genetic algorithm: NSGA-II, Evolut. Comput. IEEE Trans. 6 (2002) 182–197.

[33] T. Hemker, K. Fowler, M. Farthing, O. von Stryk, A mixed-integer simulation-based optimization approach with surrogate functions in water resources management, Optimiz. Eng. 9 (2008) 341–360.

[34] A.-T. Nguyen, S. Reiter, P. Rigo, A review on simulation-based optimization methods applied to building performance analysis, Appl. Energy 113 (2014) 1043–1058.

[35] C. Diakaki, E. Grigoroudis, D. Kolokotsa, Towards a multi-objective optimization approach for improving energy efficiency in buildings, Energy Build. 40 (2008) 1747–1754.

[36] H. Ishibuchi, Y. Shibata, Mating scheme for controlling the diversity-convergence balance for multiobjective optimization, in: K. Deb (Ed.), Genetic and Evolutionary Computation—GECCO 2004, vol. 3102, Springer, Berlin Heidelberg, 2004, pp. 1259–1271.

[37] Y.-H. Lin, Y.-P. Chen, M.-D. Yang, T.-C. Su, Multiobjective optimal design of sewerage rehabilitation by using the nondominated sorting genetic algorithm-II, Water Res. Manag. (2015) 1–17.